INSTITUTE OF PHYSICS PUBLISHING JOURNAL OF PHYSICS: CONDENSED MATTER

J. Phys.: Condens. Matter **15** (2003) 2045–2052 PII: S0953-8984(03)56176-8

Study of vibrational and magnetic excitations in $Ni_cMg_{1-c}O$ solid solutions by Raman spectroscopy

E Cazzanelli[1], A Kuzmin[2], G Mariotto[3] and N Mironova-Ulmane[2]

[1] INFM and Dipartimento di Fisica, Università della Calabria, I-87036 Arcavacata di Rende (Cosenza), Italy
[2] Institute of Solid State Physics, Kengaraga Street 8, LV-1063 Riga, Latvia
[3] INFM and Dipartimento di Fisica, Università di Trento, I-38050 Povo (Trento), Italy

E-mail: a.kuzmin@cfi.lu.lv

Received 15 November 2002
Published 17 March 2003
Online at stacks.iop.org/JPhysCM/15/2045

Abstract

The Raman scattering by phonons and magnons was studied for the first time in the polycrystalline solid solutions $Ni_cMg_{1-c}O$. The experimental Raman spectrum for $c = 0.9$ is similar to that of NiO and consists of six well resolved bands, whose origins are the disorder-induced one-phonon scattering (bands at 400 and 500 cm^{-1}), two-phonon scattering (bands at 750, 900, and 1100 cm^{-1}), and two-magnon scattering (the broad band at $\sim$1400 cm^{-1}). We found that the dependence of the two-magnon band in solid solutions on the composition and temperature is consistent with their magnetic phase diagram. We also observed that the relative contribution of two-phonon scattering decreases strongly upon dilution with magnesium ions and disappears completely at $c < 0.5$. Such behaviour is explained in terms of a disorder-induced effect, which increases the probability of the one-phonon scattering processes.

1. Introduction

Diluted antiferromagnets represent an interesting class of materials, whose crystallographic structure is closely related to their magnetic properties [1]. Recently, a correlation between long- and short-range order in solid solutions with a face-centred-cubic (fcc) magnetic sublattice has been reviewed for a number of zinc-blende- and rock-salt-type compounds [2]. In these systems, depending on the type of the host-lattice packing, the cation/anion radii ratio, and the difference in substituting ions size, the ordered-on-average crystal lattice experiences local distortions.

The $Ni_cMg_{1-c}O$ system provides a nice example of a diluted antiferromagnet. It forms a continuous series of solid solutions, whose magnetic properties vary with the composition from antiferromagnetic-like behaviour, with the Néel temperature $T_N = 523$ K for pure NiO,

to paramagnetic-like behaviour, for pure MgO [3, 4]. For intermediate compositions with $c > 0.3$, the paramagnetic-to-antiferromagnetic phase transition occurs upon cooling [3, 4].

Due to a small difference (about 0.02 Å) of the ionic radii of Ni^{2+} and Mg^{2+} ions, they can readily substitute for each other, and it has been believed for a long time [4] that the lattice parameter of the $Ni_cMg_{1-c}O$ system depends linearly on the composition, following Vegard's rule [4–8]. However, recent structural investigation by x-ray absorption spectroscopy [9, 10] and x-ray diffractometry [11] showed that nickel ions move off-centre upon dilution with magnesium ions. A symmetry lowering at Ni^{2+} sites, due to its off-centre displacement, allowed interpretation of the optical luminescence data [12] and the near-edge region in the Ni K-edge x-ray absorption spectra [13] of $Ni_cMg_{1-c}O$ solid solutions.

One can expect a dilution with magnesium and a displacement of nickel ions in $Ni_cMg_{1-c}O$ solid solutions to influence the phonon subsystem, which can be probed by Raman spectroscopy. To the best of our knowledge, until now there was no work published on this topic. Most Raman studies have been related to pure NiO [14–19] or MgO [20, 21] compounds with two exceptions [22, 23]. In [22] two-magnon Raman scattering in calcium-doped NiO with calcium concentration up to 6 mol% was investigated, whereas theoretical and experimental Raman scattering studies of impurity-induced vibrations were performed on $MgO:0.25Co^{2+}$ in [23]. The temperature-dependent [14, 15, 17–19] and pressure-dependent [16] Raman scattering in pure NiO allowed identification of contributions from one-phonon (TO and LO modes) and two-phonon (2TO, TO + LO, and 2LO modes) excitations as well as one-, two-, and four-magnon excitations. It was also found [14] that the intensity of one-phonon scattering, in particular the LO mode at $\sim$550 cm^{-1}, increases dramatically in black NiO, where the nickel vacancy concentration is high. The magnon contribution in NiO increases with decrease of temperature [14, 15, 19] or increase of pressure [16]. In calcium-doped NiO the two-magnon band broadens when calcium concentration increases [22]. Such behaviour of the magnetic subsystem agrees well with that predicted by the theory of light scattering by magnons [24, 25]. In pure MgO single crystals [20], having regular rock-salt structure, no first-order Raman effect can be detected, but the second-order Raman scattering was clearly observed. However, addition of a small amount (0.25 mol%) of cobalt ions gives rise to one-phonon bands at 278.5, 304.8, 373.8, and 421.4 cm^{-1} [21], which superimpose on the two-phonon spectrum of MgO and have comparable intensity.

In this paper, we present for the first time a Raman spectroscopy study of polycrystalline $Ni_cMg_{1-c}O$ solid solutions over a wide range of compositions, going from $c = 1$ to 0.3. Contributions from phonon and magnon scattering in the Raman spectra will be identified, and the variation of the spectra with composition and temperature will be discussed.

2. Experimental details

Polycrystalline solid solutions $Ni_cMg_{1-c}O$ ($c = 0.3, 0.4, 0.5, 0.6, 0.7, 0.9$) were prepared using ceramic technology from the appropriate amounts of aqueous solutions of $Mg(NO_3)_2{\cdot}6H_2O$ and $Ni(NO_3)_2{\cdot}6H_2O$ salts, which were mixed and slowly evaporated. The remaining dry 'flakes' were heated up to 500–600 °C to remove NO_2 completely. The polycrystalline solid solutions obtained were pressed and annealed for 100 h at $T_{an} = 1200$ °C in air and then quickly cooled down to room temperature. The pure polycrystalline NiO and MgO were obtained using the same method by thermal decomposition of the above-mentioned salts. Annealing for several NiO samples was also performed at the lower temperatures $T_{an} = 600$ and 1000 °C. These $Ni_cMg_{1-c}O$ solid solutions have greenish colour, whose intensity depends on the nickel content. Pure NiO has green colour, and pure MgO is colourless.

Room temperature Raman measurements were performed in back-scattering geometry using a micro-Raman set-up, consisting of an Olympus microscope (model BHSM-L-2), mounting an objective 80× with a numerical aperture $N_A = 0.75$ and coupled to a 1 m focal length double Jobin-Yvon monochromator (Ramanor, model HG2-S) equipped with holographic gratings (2000 grooves mm^{-1}). The spectral resolution was of the order of 3 cm^{-1}. The scattered radiation was detected by a cooled (−35 °C) photomultiplier tube (RCA, model C31034A-02), operated in the photon counting mode. The signal was stored into a multichannel analyser and then sent to a microcomputer for analysis. The Raman spectra were excited by the 488.0 nm line of an argon laser, operated so that the power entering the microscope was maintained at 20 mW.

The temperature-dependent (10–300 K) measurements were carried out in the standard macro-Raman configuration with a right-angle scattering geometry. The spectra were excited by the 514.5 nm line of an argon laser, with a nominal power of 160 mW at the cryostat window. The monochromator and detection system were the same as those used for the micro-Raman experiments. The samples were mounted in a liquid helium flux cryostat, and the temperature was controlled within ±2 K.

Our samples were polycrystalline and randomly oriented, so the polarization setting was not selective as it usually is for single crystals. However, all Raman spectra, in both micro-Raman and macro-Raman configurations, were carried out in V–V polarization, i.e. with incident and scattered radiation polarized in the same direction. Here V indicates the polarization axis of the analyser plate, which was oriented so that it fitted with the direction of the maximum efficiency of the double-monochromator gratings.

3. Results and discussion

The room temperature Raman spectrum of pure NiO consists of several bands: a one-magnon (1M) band at 34 cm^{-1} [17], five vibrational bands [15]—one-phonon (1P) TO (at 440 cm^{-1}) and LO (at 560 cm^{-1}) modes, two-phonon (2P) 2TO modes (at 740 cm^{-1}), TO + LO (at 925 cm^{-1}) and 2LO (at 1100 cm^{-1}) modes, and a two-magnon (2M) band at ∼1400 cm^{-1}. The frequency and shape of the phonon bands do not vary with temperature, whereas the magnon scattering intensities are strongly temperature dependent—they shift to lower frequencies and decrease in intensity with increasing temperature, disappearing completely close to the Néel point $T_N = 523$ K [15, 17, 19].

First, we will consider the influence of intrinsic defects, nickel vacancies, in pure green NiO on the intensity of the Raman bands (figure 1). Raman spectra of two samples, annealed at the temperatures $T_{an} = 600$ and 1000 °C, were approximately scaled on the 2LO mode, following the approach in [15]. As a result, the main difference is observed for the spectral intensity of one-phonon and two-magnon scattering. A similar but even stronger effect was previously observed for green and black NiO [15]. It was suggested [15] that an enhancement of the first-order phonon scattering occurs in black NiO due to parity-breaking defects—nickel vacancies. In our case, we expect, in spite of both samples having green colour, the higher annealing temperature ($T_{an} = 1000$ °C) to result in a lower concentration of such defects, which is in agreement with a variation of the 1P band intensity in figure 1. This explanation is also valid for the magnon scattering-related band: higher concentration of intrinsic defects leads to lower probability of magnon scattering and results in inhomogeneous broadening of the 2M band. Since the concentration of nickel vacancies in green NiO is below 0.1% [26], one can expect even stronger modifications of the Raman spectra in $Ni_cMg_{1-c}O$ solid solutions.

Room temperature Raman spectra of polycrystalline NiO, MgO, and $Ni_cMg_{1-c}O$ ($c = 0.3$, 0.4, 0.5, 0.6, 0.7, 0.9) solid solutions are shown in figure 2. Note that all samples were annealed

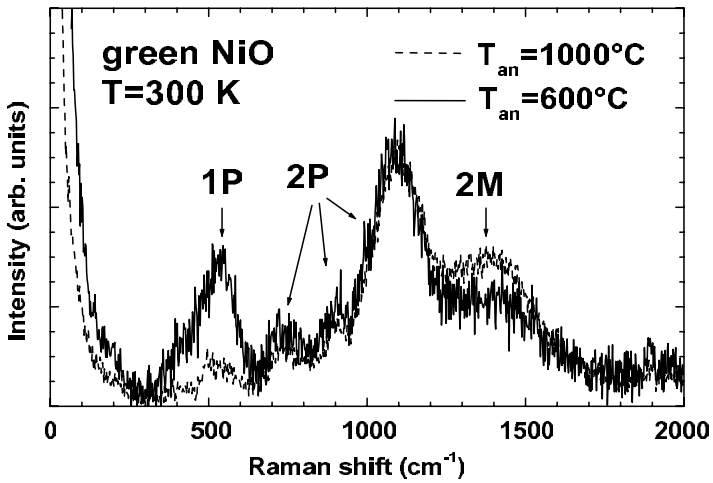

Figure 1. Room temperature (300 K) Raman spectra of green NiO polycrystalline powder, annealed at two different temperatures, 600 and 1000 °C. The spectra are normalized relative to the peak at 1100 cm^{-1} due to two-phonon (2P) scattering. Note that the intensities of two peaks, due to one-phonon (1P) and two-magnon (2M) scattering, change in opposite directions versus annealing temperature.

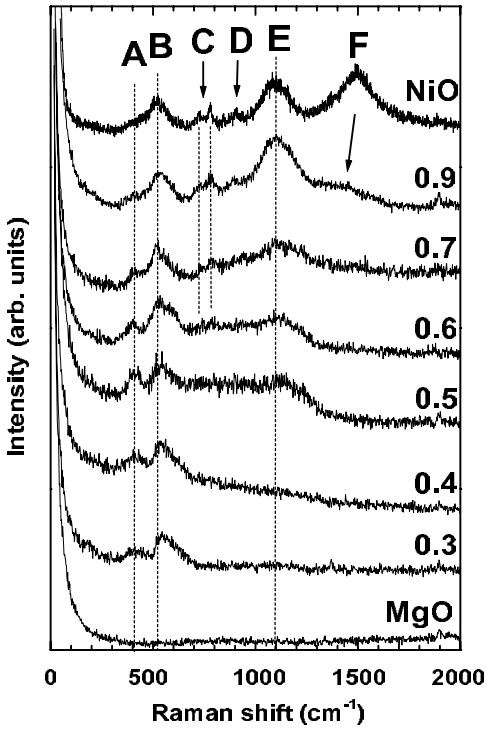

Figure 2. Room temperature Raman spectra of polycrystalline NiO, MgO, and $Ni_cMg_{1-c}O$ (c = 0.3, 0.4, 0.5, 0.6, 0.7, 0.9) solid solutions. The origin of the peaks A–F is explained in the text. The spectral intensities are scaled so that the one-phonon scatterings in the different spectra turn out roughly comparable.

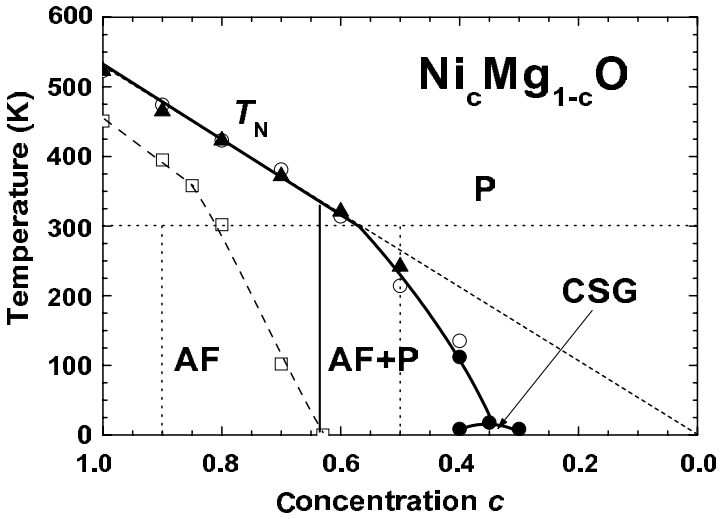

Figure 3. A magnetic phase diagram of the $Ni_cMg_{1-c}O$ system, according to elastic magnetic neutron scattering [3] and SQUID magnetometry [4]. Four regions are known: paramagnetic (P), homogeneous antiferromagnet (AF), frustrated antiferromagnet (AF + P), and cluster spin glass (CSG). The border of the region of infinite antiferromagnetic clusters is indicated by open squares [27]. The horizontal and two vertical dotted lines indicate composition- and temperature-dependent measurements, performed in the present work.

at $T_{an} = 1200\,^{\circ}C$, due to some difference being observed between spectra of pure NiO in figures 1 and 2. The six visible bands are labelled in pure NiO from A to F for convenience. Note also that our Raman spectrum for polycrystalline MgO does not show any detectable band, in contrast to what is observed for single crystals [20, 21]. This suggests a very low intensity of two-phonon scattering in MgO compared to that in NiO, so the nickel oxide sublattice is mainly responsible for the Raman scattering in our solid solutions.

According to the magnetic phase diagram of the $Ni_cMg_{1-c}O$ solid solutions (figure 3) [3, 4], the antiferromagnetic-to-paramagnetic phase transition takes place at room temperature for $c \sim 0.6$ [28]. Therefore we do not expect to see 2M scattering for more dilute samples. The band F, attributed to 2M scattering in pure NiO, broadens and shifts to lower frequencies upon dilution with magnesium as expected [22]. It becomes undetectable in our experiment for $c < 0.7$ due to a strong inhomogeneous broadening induced by the presence of magnesium ions and by the partial overlap with the two-phonon band E. It is worth noting that the influence of the chemical composition on the magnon subsystem in $Ni_cMg_{1-c}O$ single crystals was studied recently using optical absorption spectroscopy [28]. It was found [28] that a contribution of short-wavelength magnons, excited at the Brillouin zone boundary, remains visible nearly up to the transition temperature T_N due to some persistence of the local magnetic order. In particular, the intensity of the 2M-assisted absorption band for $^3A_{2g}(F) \rightarrow {}^1E_g(D)$ in $Ni_{0.6}Mg_{0.4}O$ abruptly decreases above 200 K [28]. This is in agreement with our Raman results (figure 2), which do not show any significant 2M band for $c = 0.6$ at room temperature.

The most exciting result in figure 2 is concerned with the strong decrease of the two-phonon band intensity relative to the one-phonon contribution. As one can see, upon dilution with magnesium ions, the one-phonon bands A and B change slightly in shape: mainly, the band A becomes more pronounced. At the same time, the two-phonon bands C, D, and E broaden for $0.5 \leqslant c < 0.9$ and disappear completely for $c \leqslant 0.4$. Since the crystalline structure of

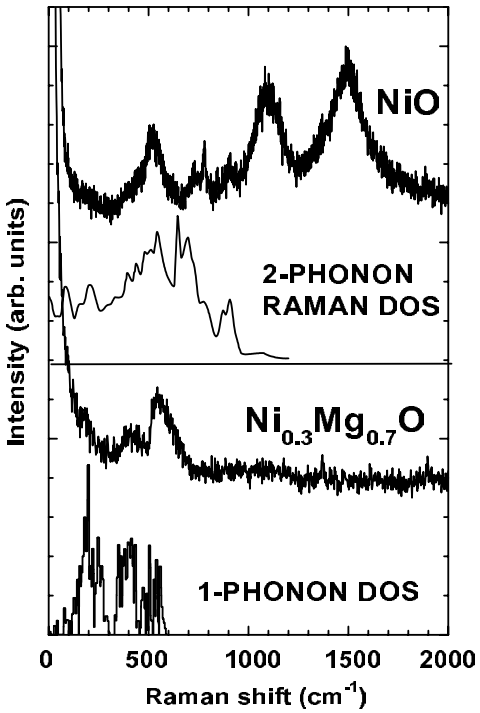

Figure 4. Room temperature Raman spectra of polycrystalline NiO and $Ni_{0.3}Mg_{0.7}O$ in comparison with the theoretically calculated one-phonon DOS [30] and two-phonon Raman DOS [29].

$Ni_cMg_{1-c}O$ solid solutions follows that of NiO and MgO (see section 1), no significant changes of the phonon density of states (DOS) are expected. Therefore, we suggest that for increasing magnesium concentration the first-order Raman scattering becomes more and more allowed due to a lowering of local symmetry at Ni^{2+} sites caused by two effects—composition disorder and off-centre displacement of nickel ions. Thus, in pure NiO and $Ni_{0.9}Mg_{0.1}O$ the first-order scattering should be forbidden, if the presence of defects is neglected. On the other hand, the solid solutions in the range of compositions $c < 0.9$ show an intermediate behaviour, in the sense that the first-order scattering of only a proportion of nickel ions remains forbidden.

To support our conclusions about the first-order Raman scattering in our solid solutions, we compare Raman spectra for pure NiO and $Ni_{0.3}Mg_{0.7}O$ with available theoretical calculations (figure 4). The two-phonon Raman DOS, calculated in [29] within the shell model, is only in relative agreement with our Raman spectrum for pure NiO. Although the positions of the peaks in the theoretical Raman DOS agree with the experimental ones, their relative intensity is rather different, especially for the 2LO band at 1100 cm^{-1}. At the other limit, in $Ni_{0.3}Mg_{0.7}O$ solid solution, the 1P band consists of two peaks, which can be related to two maxima in the one-phonon DOS, calculated in [30]. Thus, the change in shape of the Raman bands at 400–500 cm^{-1} provides a fingerprint for discrimination of the origin of the phonon scattering.

Finally, we will consider the temperature dependence of the Raman spectra for two compositions, $c = 0.9$ and 0.5 (figure 5). In both cases, variation of the temperature does not change the phonon bands significantly. The intensity of the 2M band in $Ni_{0.9}Mg_{0.1}O$ solid solution decreases with increasing temperature as expected [14]. However, even at 10 K, the 2M band for $c = 0.9$ is much broader than that for pure NiO [14], because of a relevant

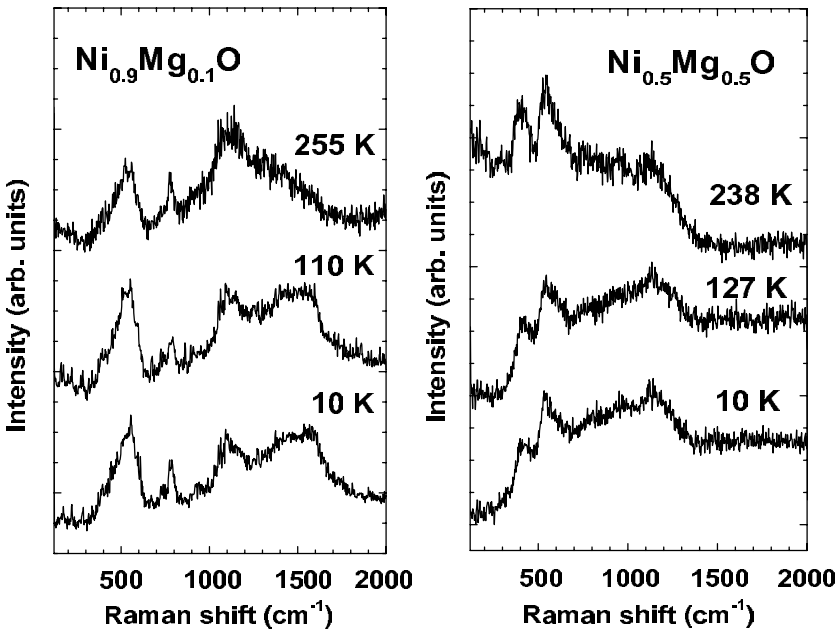

Figure 5. Temperature dependences of the Raman scattering in $Ni_{0.9}Mg_{0.1}O$ and $Ni_{0.5}Mg_{0.5}O$ solid solutions. Only few spectra are shown for clarity. Note a change of the background of the Raman signals from $Ni_{0.5}Mg_{0.5}O$.

inhomogeneous broadening induced by magnesium ions. At the same time, no resolved 2M band is observed for $Ni_{0.5}Mg_{0.5}O$ solid solution even at 10 K. It seems that in this case, the 2M band is located under the phonon bands and could be partially responsible for the background contribution, which becomes negligible above ∼150 K. One can estimate the energy position of the 2M band in both solid solutions from an Ising cluster model, developed in [31] and applied previously to NiO doped with calcium in [22]. According to the model [31], the position $\omega(2M)$ of the 2M band in antiferromagnetic mixed crystals containing non-magnetic ions changes linearly with composition: $\omega(2M) = 2zJ_{NNN}S(1 - (1 - c)(z - 1)/z) - J_{NNN}$ where $z = 6$ is the number of next-nearest neighbours (NNN), J_{NNN} is the superexchange interaction energy within $180°Ni^{2+}$–O^{2-}–Ni^{2+} atomic chains, and $S = 1$ is the spin. Note that this expression neglects the weaker ferromagnetic-type 90° nearest-neighbour interactions [32] and percolation effects [4], and assumes a constant value [13] of the superexchange energy J_{NNN} at all compositions. For pure NiO ($c = 1$) at 10 K, $\omega(2M) = 1554\ cm^{-1}$ [14, 22] and $J_{NNN} = 141.3\ cm^{-1}$. Using this value of J_{NNN}, one obtains $\omega(2M) = 1413\ cm^{-1}$ for $c = 0.9$ and $\omega(2M) = 848\ cm^{-1}$ for $c = 0.5$. As one can see in figure 5, the prediction for $Ni_{0.9}Mg_{0.1}O$ is in good agreement with the experiment. In the case of $Ni_{0.5}Mg_{0.5}O$, the estimate for $\omega(2M)$ supports our conclusion that the two-magnon contribution is located under the phonon bands.

4. Conclusions

Raman scattering by phonons and magnons was studied for the first time in the polycrystalline solid solutions $Ni_cMg_{1-c}O$. On the basis of the magnetic phase diagram [3, 4], the composition dependence of the Raman spectra was studied at room temperature, whereas their temperature dependences were followed for two compositions, $c = 0.9$ and 0.5.

A comparison of the Raman spectra from solid solutions with those of pure NiO and MgO allowed us to draw several conclusions. First, the two-magnon band is visible for $c > 0.6$ at room temperature and below the Néel temperature for $c = 0.9$ and 0.5. This is in good agreement with the magnetic phase diagram of $Ni_cMg_{1-c}O$ system [3, 4]. Second, upon dilution with magnesium, a relative increase of one-phonon scattering is observed, whereas the two-phonon contribution seems to disappear completely at $c < 0.5$. This phenomenon is explained in terms of the local symmetry lowering at Ni^{2+} sites, caused by chemical substitution and off-centre displacement of nickel ions [9–11].

In addition to the two-magnon scattering, a one-magnon contribution is also known to exist in pure NiO [17, 19]. In comparison to the two-magnon excitations, which are due to short-range magnetic interactions at the Brillouin zone boundary, the one-magnon excitations, occurring at the Brillouin zone centre, are expected to be more sensitive to the compositional disorder. Therefore, their study in solid solutions is of great interest, and is in fact in progress.

Acknowledgments

AK is grateful to the University of Trento and to the CeFSA Laboratory of ITC-CNR (Trento) for hospitality and financial support. This work was supported in part by the Latvian Government Research Grants Nos 01.0821 and 01.0806.

References

[1] Furdyna J K and Kossut J (ed) 1988 *Diluted Magnetic Semiconductors* (New York: Academic)
[2] Kuzmin A 1997 *Disorder Mater. Newslett.* **11** 1
[3] Menshikov A Z, Dorofeev Yu A, Klimenko A G and Mironova N A 1991 *Phys. Status Solidi* b **164** 275
[4] Feng Z and Seehra M S 1992 *Phys. Rev.* B **45** 2184
[5] Hahn W C and Muan J A 1961 *J. Phys. Chem. Solids* **19** 338
[6] Mironova N A and Bandurkina G V 1975 *Izv. Akad. Nauk Latv. SSR, Ser. Fiz. Tekh. Nauk* **4** 14
[7] Hagan A P, Lofthouse M G, Stone F S and Trevethan M A 1979 *Preparation of Catalysts* vol 2 (Amsterdam: Elsevier) p 417
[8] Yoshida T, Tanaka T, Yoshida H, Funabiki T and Yoshida S 1996 *J. Phys. Chem.* **100** 2302
[9] Kuzmin A, Mironova N, Purans J and Rodionov A 1995 *J. Phys.: Condens. Matter* **7** 9357
[10] Mironova N, Kuzmin A, Purans J and Rodionov A 1995 *Proc. SPIE* **2706** 168
[11] Kuzmin A and Mironova N 1998 *J. Phys.: Condens. Matter* **10** 7937
[12] Mironova N, Skvortsova V, Kuzmin A and Purans J 1997 *J. Lumin.* **72–74** 231
[13] Kuzmin A, Mironova N and Purans J 1997 *J. Phys.: Condens. Matter* **9** 5277
[14] Dietz R E, Parisot G I and Meixner A E 1971 *Phys. Rev.* B **4** 2302
[15] Dietz R E, Brinkman W F, Meixner A E and Guggenheim H J 1971 *Phys. Rev. Lett.* **27** 814
[16] Massey M J, Chen N H, Allen J W and Merlin R 1990 *Phys. Rev.* B **42** 8776
[17] Lockwood D J, Cottam M G and Baskey J H 1992 *J. Magn. Magn. Mater.* **104–107** 1053
[18] Grimsditch M, Kumar S and Goldman R S 1994 *J. Magn. Magn. Mater.* **129** 327
[19] Grimsditch M, McNeil L E and Lockwood D J 1998 *Phys. Rev.* B **58** 14462
[20] Manson N B, Von der Ohe W and Chodos S L 1971 *Phys. Rev.* B **3** 1968
[21] Pasternak A, Cohen E and Gilat G 1974 *Phys. Rev.* B **9** 4584
[22] Funkenbusch E F and Cornilsen B C 1981 *Solid State Commun.* **40** 707
[23] Guha S 1980 *Phys. Rev.* B **21** 5808
[24] Stevens A 1972 *J. Phys. C: Solid State Phys.* **5** 1859
[25] Cottam M G and Awang A L 1979 *J. Phys. C: Solid State Phys.* **12** 105
[26] Finster J, Lorenz P, Fiévet F and Figlarz M 1982 *Proc. 9th Int. Symp. on Reactivity of Solids (Krakov)* p 303
[27] Mironova N A, Belyaeva A I, Miloslavskaja O V and Bandurkina G V 1981 *Ukr. Fiz. Zh.* **34** 848
[28] Mironova-Ulmane N, Skvortsova V, Kuzmin A and Sildos I 2002 *Phys. Solid State* **44** 1463
[29] Reichardt W, Wagner V and Kress W 1975 *J. Phys. C: Solid State Phys.* **8** 3955
[30] Kushwaha M S 1982 *Physica* B **112** 232
[31] Buchanan M, Buyers W J L, Elliot R J, Harley R T, Hayes W, Perry A M and Saville I D 1972 *J. Phys. C: Solid State Phys.* **5** 2011
[32] Seehra M S and Giebultowicz T M 1988 *Phys. Rev.* B **38** 11898